

1 **Mechanistic model of temperature influence on flowering through whole-plant**
2 **accumulation of *FT***

3 **Running title:** Modeling phenology through *FT* transcription and accumulation

4

5 Hannah A. Kinmonth-Schultz^{1,a}, Melissa J. MacEwen^{1,b}, Daniel D. Seaton^{2,c}, Andrew J.
6 Millar^{2,d}, Takato Imaizumi^{1,e}, Soo-Hyung Kim^{3,f}

7

8 ¹Department of Biology, University of Washington, Seattle, WA 98195-1800, USA

9 ²SynthSys and School of Biological Sciences, University of Edinburgh, Edinburgh EH9 3BF,
10 UK

11 ³School of Environmental and Forest Sciences, University of Washington, Seattle, WA 98195-
12 2100, USA

13 ^ahkinmonth@uwalumni.com

14 ^bmacewm@uw.edu

15 ^cdseaton@ebi.ac.uk

16 ^dandrew.millar@ed.ac.uk

17 ^etakato@uw.edu

18 ^fAuthor for correspondence: Soo-Hyung Kim

19 Tel: +1-206-616-4971

20 Email: soohkim@uw.edu

21

22 **Highlight**

23 We examined temperature influence on transcript regulation, organ-specific whole-plant *FT*
24 accumulation, and flowering time using the *Arabidopsis* Framework Model. We also quantified
25 *FT*'s changing systemic interactions throughout development.

26

27 **Abstract**

28 We assessed temperature influence on flowering by incorporating temperature-responsive
29 flowering mechanisms across developmental age into an existing model. Temperature influences
30 both the leaf production rate and expression of *FLOWERING LOCUS T (FT)*, a photoperiodic
31 flowering regulator, in leaves. The *Arabidopsis* Framework Model incorporated temperature
32 influence on leaf growth but ignored the consequences of leaf growth on and direct temperature
33 influence of *FT* expression. We measured *FT* production in differently aged leaves and modified
34 the model, adding the mechanistic temperature influence on *FT* transcription, and linking *FT* to
35 leaf growth. Our simulations suggest that in long days, the developmental timing (leaf number)
36 at which the reproductive transition occurs is influenced by day length and temperature through
37 *FT*, while temperature influences the rate of leaf production and the time (in days) the transition
38 occurs. Further, we demonstrated that *FT* is mainly produced in the first 10 leaves in the
39 Columbia ecotype, and that *FT* accumulation alone cannot explain flowering in conditions in
40 which flowering is delayed. Our simulations supported our hypotheses that: 1) temperature
41 regulation of *FT*, accumulated with leaf growth, is a component of thermal time, and 2)
42 incorporating mechanistic temperature regulation of *FT* can improve model predictions in
43 fluctuating temperatures.

44

45 **Key words:** *Arabidopsis thaliana*, flowering time, *FT*, phenology, temperature fluctuation,
46 thermal time, crop simulation model, mathematical model

47

48

49

50 **Introduction**

51 Ambient temperature during the growing season correlates with the timing of plants' transition
52 from vegetative to reproductive growth. Germination, organ emergence, leaf expansion,
53 photosynthesis, and respiration display similar relationships (Parent *et al.*, 2010). These findings
54 have led to the concept of "thermal time" (Lehenbauer, 1914), a metric that asserts that
55 temperature-driven metabolic rates govern development (Zavalloni *et al.*, 2006), and to models
56 that use the empirical relationship between temperature and development to predict plant
57 response (e.g., Chuine, 2000; Jones *et al.*, 2003).

58 Thermal time accumulation describes an aggregate of underlying plant responses. Thermal units
59 accumulate more quickly, and reach a predetermined threshold sooner to predict flowering,
60 during warm growing seasons than cool ones. Thermal time implies 1) that all plant
61 physiological rates increase in tandem with temperature increases and 2) that fluctuating and
62 constant temperatures have the same influence on most physiological rates if the mean
63 temperature remains stable. However, processes do not always slow under cool temperatures.
64 The up-regulation of cryo-protective genes (Jaglo-Ottosen *et al.*, 1998) and the circadian clock's
65 buffering to temperature changes (Rensing & Ruoff, 2002) are just two examples.

66 Furthermore, predicting plant response to future climates remains imprecise when considering
67 temperature alone or in conjunction with CO₂ (Asseng *et al.*, 2013; Makowski *et al.*, 2015). The
68 effect of non-stressing temperatures varies among cultivars (Karsai *et al.*, 2013), and plants may
69 respond differently to temperature fluctuations than predicted from constant temperatures (Yin &
70 Kropff, 1996; Kim *et al.*, 2007; Karsai *et al.*, 2008). As most plant models incorporate some
71 variant of thermal time (Ritchie & Otter, 1985; Jamieson *et al.*, 1998a,b; Wilczek *et al.*, 2009; He
72 *et al.*, 2012; Kumudini *et al.*, 2014), they may fail to capture aspects of temperature response.
73 Differing day-length or climate responses may also confound model prediction, with the same
74 cultivar showing different thermal-time requirements, depending on planting date, location, or
75 growth conditions (Piper *et al.*, 1996; Kumudini *et al.*, 2014; Carter *et al.*, 2017). Incorporating
76 the molecular mechanisms of cultivar response in different environments should improve
77 models' predictive capacity.

78 A more mechanistic approach would decompose environmental influences into separate model
79 processes (Welch *et al.*, 2003; Kim *et al.*, 2012; Zheng *et al.*, 2013; Brown *et al.*, 2013). One

80 such approach, in wheat, noted that the number of leaves produced before the reproductive
81 transition decreased as the environmental signal's strength increased (Jamieson *et al.*, 1998b).
82 Prolonged cold, vernalizing temperatures followed by longer days reduced the leaf number at
83 which the transition occurred, while ambient temperature influenced the rate the leaves were
84 produced (Brown *et al.*, 2013). Modeling accumulation of *VRN3*, a key flowering gene, in
85 response to vernalization and day length cues, and as a function of thermal time, accurately
86 predicted final leaf number and timing of flowering (Brown *et al.*, 2013).

87 *VRN3* is an orthologue of *FLOWERING LOCUS T (FT)* in *Arabidopsis thaliana* (Yan *et al.*,
88 2006), an integrator of environmental cues in the photoperiodic flowering pathway (Song *et al.*,
89 2015). *FT* levels correlate strongly with the leaf number present when flowering occurs
90 (Krzymuski *et al.*, 2015; Seaton *et al.*, 2015; Kinmonth-Schultz *et al.*, 2016). In turn, day length,
91 vernalization, and ambient temperature changes regulate *FT* expression (Blazquez *et al.*, 2003;
92 Amasino, 2010; Song *et al.*, 2015). *FT* simulated as a function of day length and accumulated as
93 a function of thermal time can accurately predict flowering in some conditions (Chew *et al.*,
94 2012). Under constant and fluctuating temperature conditions, cool temperatures suppress *FT*
95 through the interaction of SHORT VETIGATIVE PHASE (SVP) and the FLOWERING LOCUS
96 M (FLM)- β splice variant on the *FT* regulatory regions (Blazquez *et al.*, 2003; Posé *et al.*, 2013;
97 Lee *et al.*, 2013; Lutz *et al.*, 2015; Sureshkumar *et al.*, 2016; Kinmonth-Schultz *et al.*, 2016).
98 However, temperature fluctuations from warm to cool induce *FT* through induction of
99 *CONSTANS (CO)*, a chief transcriptional activator of *FT* (Schwartz *et al.*, 2009; Kinmonth-
100 Schultz *et al.*, 2016). As there is no simple correlation between temperature decrease and *FT*
101 level reduction, the linear accumulation of flowering gene products with thermal time may not
102 adequately capture the influence of temperature on final leaf number, especially in fluctuating
103 temperatures.

104 Further, *FT* protein is expressed in the leaves and moves to the shoot apex where it complexes
105 with FLOWERING LOCUS D (FD) protein to induce the transition from leaf to floral
106 production (Abe *et al.*, 2005; Corbesier *et al.*, 2007). The amount of *FT* protein perceived at the
107 shoot apex likely depends on the amount of leaf tissue present. Leaf production and growth are
108 strongly temperature dependent (Parent *et al.*, 2010). We proposed that a key mechanism
109 underlying thermal time accumulation could be either the accumulation of gene product (e.g., *FT*

110 protein) or the increasing capacity for transcript production as a plant grows. In either case, the
111 rate of FT accumulation would be further adjusted by day length and by direct temperature
112 influence on *FT* gene expression.

113 To predict whole-plant *FT* accumulation we must consider changes in *FT* expression with
114 developmental age. Likely, *FT* expression is not consistent in all leaves or developmental stages.
115 The transcriptional reporter, *pFT:GUS* was expressed in the tips of the two true leaves in six-
116 day-old seedlings, but ranged across the leaf in 12-day-old plants having five to seven true leaves
117 (Takada & Goto, 2003). Further, whole-plant transcript levels increase from age five to 15 days
118 relative to an internal control, indicating changing capacity for *FT* expression with age (Mathieu
119 *et al.*, 2009). *FT* transcript levels have neither been measured in leaves of different ages, nor has
120 this been considered in flowering models, but it could improve our understanding of how day
121 length and temperature impact *FT* to control flowering across developmental age.

122 In earlier work we found *FT* levels correlate with flowering across a range of temperature
123 conditions ((Kinmonth-Schultz *et al.*, 2016). We also observed that *FT* can be both induced and
124 suppressed by cool temperatures depending on whether constant or fluctuating temperatures are
125 applied (Kinmonth-Schultz *et al.*, 2016). This provided us with an opportunity to determine the
126 relative influences of *FT* transcriptional control versus whole-plant *FT* accumulation via leaf
127 production. One possibility is that despite *FT* induction by a temperature drop, flowering would
128 be delayed because whole-plant leaf production is slowed. Alternatively, *FT* induction could
129 result in flowering times that are earlier than predicted. To address these questions we utilized an
130 existing model (The *Arabidopsis* Framework Model; FM-v1.0) capable of simulating plant
131 growth and flowering times in response to temperature (Chew *et al.*, 2014). We assessed FM-
132 v1.0's capacity to simulate growth in fluctuating temperature conditions. We then quantified the
133 level of *FT* produced in leaves of different ages and built new models describing the behavior of
134 *FT* across leaves and the influence of fluctuating temperatures on *FT*. We integrated these
135 models into FM-v1.0, linking *FT* accumulation to leaf tissue production. Using this altered
136 model, referred to as FM-v1.5, we explored the sensitivity of *FT* accumulation to both gene
137 expression and leaf growth, and demonstrated how each component may influence flowering
138 times. FM-v1.0 used a more traditional thermal-time approach to determine flowering times,
139 whereas FM-v1.5 uses a more mechanistic approach based on *FT* levels, hence we also

140 compared mechanistic and thermal-time methods of simulating temperature influence on
141 flowering.

142

143 **Material and Methods**

144 *Description of Arabidopsis Framework Model and Modifications*

145 The *Arabidopsis* Framework Model (FM-v1.0, Figure S1, Chew *et al.*, 2014) combines plant
146 growth and mechanistic flowering regulation for *Arabidopsis*. FM-v1.0 is run in two phases. In
147 phase one, the timing of flowering is determined by thermal time accumulation ($T(t) - T_{base}$,
148 calculated hourly) in the Phenology module, with daytime temperature given more weight
149 (Wilczek *et al.*, 2009; Chew *et al.*, 2012). Thermal time is modified by day length, to produce
150 Modified Photothermal Units (MPTUs), through mechanistic circadian- and day-length *FT*
151 transcriptional regulation in the Photoperiodism module (Salazar *et al.*, 2009). The number of
152 days required to reach the MPTU threshold determines the stopping point of vegetative growth
153 and onset of flowering, and is used as an input in phase two. In phase two, the climate
154 parameters affect vegetative growth. Growth is determined by the rate of photosynthesis and
155 carbon partitioning between roots and shoots (Carbon Dynamic module, Rasse & Tocquin,
156 2006), and includes the rate of organ production as a function of thermal time, including
157 production of individual leaves (Functional Structural Plant module, Christophe *et al.*, 2008). To
158 modify FM-v1.0, we removed the thermal time accumulation used in phase one of FM-v1.0 and
159 instead incorporated mechanistic temperature influence on *FT* into the Photoperiodism module.
160 We maintained thermal time control over leaf tissue production in phase two, but modified the
161 SLA and respiration components to improve the response of leaf growth to fluctuating
162 temperatures. Then, rather than running the model in two phases, we called the Phenology and
163 Photoperiodism modules at each time step, considering their outputs *FT* gene expression per unit
164 of leaf tissue. We used the leaf number, age, and area outputs at each time step to determine the
165 relative *FT* produced by each leaf, and summed the value of *FT* across all leaves to get a whole-
166 plant *FT* value. Our modifications (FM-v1.5, Figure 1) are described in detail below.

167

168 1. *FT transcript accumulation in fluctuating temperatures simulated through SVP and CO*
169 *influence*

170 Under long days (LD), in 22 °C day, 12 °C night temperature-cycle conditions (22°C /12 °C-
171 night), *FT* was suppressed at dusk compared to 22 °C constant temperatures (22°C-constant)
172 (Kinmonth-Schultz et al. 2016) likely through the action of SVP and the FLM-β splice variant,
173 consistent with prior observations under constant temperatures (Blazquez *et al.*, 2003; Lee *et al.*,
174 2007, 2013; Posé *et al.*, 2013). SVP protein levels increased shortly after exposure to cool
175 temperatures (Kinmonth-Schultz et al. 2016), as did the ratio of *FLM-β* to *FLM-δ* splice variants
176 (Posé *et al.*, 2013). FLM-β facilitates SVP binding, and SVP and FLM-β protein levels increase
177 with decreasing temperatures (Lee *et al.*, 2013). Both SVP and FLM-β are present at 23 °C; a
178 transfer from 23 °C to 27 °C resulted in SVP decay that occurred within 12 h (Lee *et al.*, 2013).
179 We used a single term to simulate the combined SVP and FLM-β behavior termed “SVP
180 activity”. Consistent with the observed behavior of these proteins, we modeled SVP activity to
181 increase in response to a decrease in temperature, as shown below.

182 [1.1]
$$SVP_{new}(t) = \min \left\{ SVP_{mx}, \max \left[0, \left(a - \exp(-VT_{SVP}T(t)) \right) \right] \right\}$$

183 [1.2]
$$SVP_{mx} = \exp(-b \cdot d_{FTL})$$

184 SVP_{new} is the newly synthesized protein (nmol/h), VT_{SVP} describes the degree SVP synthesis
185 decreases in response to a temperature increase, the intercept (a) is used to adjust the overall
186 amount of SVP synthesized, T is temperature (°C), and t is time ($t = 0$ at sowing). The influence
187 of SVP may decline over time, as cool-temperature suppression of *FT* disappeared over a two-
188 week period (Figure S2a-b). To simulate this, SVP_{mx} declines relative to days post emergence of
189 the first true leaves (d_{FTL} , eq. [1.2], Figure S2c). SVP_{new} is synthesized every hour, and is input
190 into a differential equation calculated continuously [1.3]. Values and units of each coefficient are
191 in Table S1. To capture the suppression of *FT* at dusk, we set the SVP decay rate to be slightly
192 lower than its production. This caused SVP to remain higher at 22 °C after a 12 °C night than in
193 22°C-constant conditions, even after several hours (Figure S2c). The decay rate (v_{SVP}) is
194 proportional to the present SVP concentration.

195 [1.3]
$$\frac{dSVP}{dt} = SVP_{new} - (v_{SVP} \cdot SVP)$$

196 In LD 22°C /12°C-night, *FT* levels are higher at dawn coinciding with higher *CO* mRNA and
 197 protein in cool nights (Kinmonth-Schultz *et al.*, 2016). While SVP activity may respond to
 198 absolute changes in temperature (Lee *et al.*, 2007, 2013; Posé *et al.*, 2013), *CO* accumulation is
 199 induced by rapid changes from warm to cool (Kinmonth-Schultz *et al.*, 2016). The degree of
 200 temperature change is likely a factor, as a drop of 10 °C (22°C /12°C-night) yielded more *CO*
 201 transcript accumulation than did a drop of 5 °C (22°C/17°C-night) relative to 22 °C constant
 202 temperatures (Kinmonth-Schultz *et al.*, 2016). This relationship was linear across the three
 203 treatments (Figure S3a). We correlated *CO* mRNA induction (*KT*) linearly with the difference
 204 (*dT*) between the maximum and current temperatures (eq. [1.4]). To determine *dT*, the model
 205 queries the temperature at each time step, and compares the current temperature against the
 206 previous maximum temperature. If higher, the current temperature is set as the new maximum
 207 temperature. *dT* may be zero if there has been no decrease in temperature, and *KT* cannot fall
 208 below zero.

209 [1.4]
$$KT = \max \left\{ 0, \left[1 + \left(KT_o \cdot dT \cdot \exp(-c(d_{dT})) \right) \right] \right\}$$

210 Coefficient *c* describes the rate at which *CO* induction changes with *dT*. The influence of a
 211 temperature change fades over several days if the temperature remains cool over that timeframe
 212 (Figure S3b). To account for this, *d_{dT}* is the time (days) since the change in temperature occurred.
 213 *KT* is used to modify the *CO* mRNA (*CO_m*) amount produced (eq. [1.4]), as temperature seems
 214 to influence *CO* through transcription (Kinmonth-Schultz *et al.*, 2016). *CO_m* is an input for the
 215 *CO* protein (*CO_p*) equation as in Chew *et al.*, 2014, as shown below (eq. [1.5]). Decay occurs
 216 only at night (*L₁* = Light period).

217 [1.5]
$$CO_{new} = CO_m \cdot KT$$

218

219 [1.6]
$$\frac{dCO_p}{dt} = v_{CO_{p1}}(CO_m) - v_{CO_{p2}} \frac{CO_p}{k_{CO_{p1}} + CO_p} (1 - L_1)$$

220

221 The SVP/FLM- β complex and CO may act competitively at the *FT* promoter (Bratzel & Turck,
222 2015), with CO overcoming suppression by SVP/FLM- β at night when its levels are high. The
223 Photoperiod module in FM-v1.0 (Chew *et al.*, 2014) describes the relationship between *FT*
224 transcription and CO protein (eq. [S2.1]). We incorporated the interaction between CO and
225 SVP/FLM- β using a modified Michaelis-Menten function for competitive inhibition (Segal,
226 1976), such that the k of *FT* induction by CO (k_{CO_p1}) is influenced by SVP activity as below.

227 [1.7]
$$\frac{dFT}{dt} = L_2 \cdot \left(v_{CO_{p3}} \frac{CO_p}{k_{CO_{p2}} \left(1 + \frac{SVP}{k_{SVP}} \right) + CO_p} - v_{FT_1} \frac{FT}{k_{FT_1} + FT} \right)$$

228 The lower-case v and k are Michaelis-Menten constants either describing the *FT* synthesis rate as
229 influenced by CO protein (CO_p) or SVP activity, or *FT* degradation. *CO* and *FT* induction were
230 observed when the temperature dropped both at dawn and dusk (Kinmonth-Schultz *et al.*, 2016),
231 like previous observations (Thines *et al.*, 2014). However, daytime *CO* induction was lower than
232 nighttime induction while *FT* induction was higher. The higher daytime CO protein production
233 captured in equation [1.6] was not enough to capture this behavior. While dusk regulation of *FT*
234 is well understood (Song *et al.*, 2015), the mechanisms governing the morning *FT* induction
235 sometimes observed (Corbesier *et al.*, 2007) are not known. To capture the observed behavior,
236 we increased *FT* transcriptional sensitivity in the morning (L_2) using a switch function that relied
237 on a model component that peaks around dawn, specifically the circadian clock component,
238 *LHY*, from the Photoperiodism module, (Figure S4). This enabled us to approximate the
239 observed behavior of *FT*.

240 To entrain the diurnal *FT* and *CO* patterns, we incorporated data from three different treatment
241 types all in 16-h photoperiods grown at $\sim 60 \text{ umol m}^{-2} \text{ s}^{-1}$ photon flux density: warm-day (22 °C),
242 cool-night (12 or 17 °C) temperature cycles, in which the temperature change occurred at dusk
243 (24 wild-type replicates, six including 17 °C, and five including the *svp* mutant line); constant
244 warm (22 °C) temperatures shifting to constant cool (12 or 17 °C) temperatures at dawn (eight
245 and three replicates respectively); and growth at 12 and 17 °C from seed (three replicates each)
246 (Kinmonth-Schultz *et al.*, 2016). In all instances, growth from seed at 22 °C was used as the

247 control. The temperature-cycle harvests including 17 °C spanned two days. An ANOVA
248 comparison of models including and excluding *day* as a factor, showed no difference. The days
249 were counted as separate replicates for model training. *FT* and *CO* gene expression were pooled
250 across all replicates within a treatment and normalized across treatments to the mean peak *FT*
251 expression (ZT 16) and mean peak *CO* expression (ZT 16 and 20 mean) in the 22 °C control.
252 Parameter values for change in *CO* induction and *SVP* activity over a period of days were
253 determined using experiments with four replicates each (Kinmonth-Schultz *et al.*, 2016). As we
254 were interested in the cumulative influence of *FT*, we assessed model fit and performance in
255 three ways: (1) minimizing RMSE between observed and predicted gene expression profiles over
256 the 24-h harvest period (14 d after sowing), (2) comparing observed and predicted amounts of
257 *CO* and *FT* as calculated as the area under the curve (AUC) 14 d after sowing, and (3)
258 maintenance of gene expression patterns through time.

259

260 2. Incorporating *FT* as a function of leaf and plant age

261 We found that *FT* expression declined as leaves aged. Newer leaves in older plants seemed to
262 lose capacity to express *FT* (Figure 2, S5). To simulate the proportion of *FT* per unit tissue (*FT*,
263 nmol cm⁻²) of each leaf, we used a beta function (eq. [3.1], Yin *et al.*, 1995) based on relative
264 leaf age (*r*), beginning with the youngest emerged leaf as leaf one.

265

$$266 \quad [2.1] \quad \beta_{FT} = \max \left(0, \beta_{FTmx} \left[\left(\frac{r}{R_{opt}} \right) \left(\frac{R_{crit} - r}{R_{crit} - R_{opt}} \right) \left(\frac{R_{crit} - R_{opt}}{R_{opt}} \right)^e \right] \right)$$

267 β_{FT} yields a value between zero and one. β_{FTmx} describes the maximum value that can be attained
268 by a leaf of a single plant, R_{opt} is the relative age at which that maximum value is attained, R_{crit} is
269 the oldest leaf that can express *FT*, and e describes the steepness of the curvature. This function
270 causes the dependent variable to oscillate if the independent variable spans a broad range. To
271 avoid this behavior, we set β_{FT} to be zero below and above the relative ages where β_{FT} first
272 attains a minimum. β_{FTmx} and R_{opt} are dependent on the total number of leaves on a plant (l), as

273 described below, avoiding the need to reparameterize for plants of different ages. f and g are
274 coefficients.

275 [2.2]
$$\beta_{FT_{mx}} = 1 - \left(\frac{f}{l} \right)$$

276 [2.3]
$$R_{opt} = gl$$

277

278 3. Determining whole-plant FT levels and accumulating FT to a threshold

279 To link FT transcript accumulation to leaf tissue production, the Phenology module is called at
280 each time step. We consider the output of the Phenology module to be the amount of FT
281 produced per unit leaf area (FT , nmol cm⁻²). This value is adjusted by leaf area (LA , cm²) and
282 capacity of each leaf to express FT (β_{FT} , unitless modifier), as FT induction is dependent on light
283 intercepted by the leaf.

284 [3.1]
$$FT_{leaf} = LA \cdot \beta_{FT} \cdot FT$$

285 At each time step, FT_{leaf} (nmol leaf⁻¹) is determined for each leaf, summed across all leaves, and
286 added to the value from the previous time step to determine whole-plant FT levels. Such FT
287 accumulation is consistent with the observation that several days of FT induction are needed to
288 induce flowering (Corbesier *et al.*, 2007; Krzymuski *et al.*, 2015; Kinmonth-Schultz *et al.*, 2016).
289 To predict flowering, the model runs until a threshold level of FT is reached. This threshold is
290 determined by simulating whole-plant FT , at constant 22 °C in LDs, accumulated until a target
291 leaf number is reached. All other treatments are run to this threshold under the assumption that it
292 remains conserved under different growing temperatures.

293 In FM-v1.0, the development rate towards flowering, as influenced by FT amount and
294 photoperiod, is limited below and above two critical daylengths (10 and 14 h) using a different
295 parameter set for each photoperiod (Chew *et al.*, 2014).

296 [3.2]
$$Photoperiod = A + B \left[\frac{C^n}{C^n + (FT_{area})^n} \right]$$

297 Here, we removed this function and considered direct *FT* accumulation. Determining the
298 absolute amount of *FT* required to induce flowering and whether there are threshold levels of
299 transcription, below and above which flowering time is unaffected, will be a useful future study.
300 We maintained the vernalization component from FM-v1.0 to maintain model flexibility, as
301 vernalization should modify overall levels of *FT* (Helliwell *et al.*, 2006; Searle *et al.*, 2006). This
302 value falls between zero and one and now modifies the levels of *FT* produced within the
303 Phenology model rather than modifying the thermal unit accumulation rate.

304

305 4. *Adjusting FM-v1.0 leaf-area response to fluctuating temperature*

306 FM-v1.0 was parameterized for constant temperatures. It captured the leaf areas of plants
307 exposed to different constant temperatures, but simulated larger areas for plants grown in
308 fluctuating temperatures than the constant-temperature control (Figure S6a). Observed plants
309 accumulated similar biomass, but a lower Specific Leaf Area (SLA, $\text{m}^2 \text{g}^{-1}$) under fluctuating
310 temperatures relative to a constant-temperature control (Pyl *et al.*, 2012). In FM-v1.5, we
311 adjusted the SLA and respiration components to improve the relationship among leaf areas
312 across fluctuating temperature conditions (described below).

313 The larger leaf area under fluctuating temperatures in FM-v1.0 occurred for two reasons. First,
314 SLA decreases with increasing thermal time (i.e. developmental time, Christophe *et al.* 2008). In
315 FM-v1.0, this causes simulated SLA to be lower in warmer conditions because development is
316 faster (Figure S6b-c), while all treatments begin at a similar biomass. Second, FM-v1.0 relates
317 maintenance respiration to temperature using the Arrhenius function, causing respiration to be
318 lower under cooler temperatures. Under warm daytime temperatures, plants simulated in
319 fluctuating temperatures accumulate the same amount of stored carbon as the control (Figure
320 S6d). Once shifted to cooler temperatures, the lower maintenance respiration rate (Figure S6e)
321 leaves a larger stored carbon pool that can be used for growth, causing larger leaves.

322 Respiration, carbon storage, or growth may be altered by temperature in ways not captured in the
323 model. In cold-tolerant woody species, respiration of stem cuttings increased near freezing,
324 rather than following the trend predicted by the Arrhenius function, as did the pool of non-
325 structural carbohydrates (NSC) (Sperling *et al.*, 2015). Respiration may also increase at more

326 moderate temperatures in cases where freezing tolerance is induced, as in *Arabidopsis* at 16 °C in
327 light with a low red/far-red ratio (Franklin & Whitelam, 2007). In chrysanthemum, cool
328 nighttime temperatures decreased leaf area while increasing dry weight, by increasing stored
329 starch (Heinsvig Kjær *et al.*, 2007). FM-v1.0 does not incorporate these complexities nor
330 consider sinks for carbon other than growth, such as NSCs. Therefore, to simulate the relative
331 relationships in leaf area across temperature conditions needed for our study (Figure S6f), we
332 removed the temperature sensitivity of maintenance respiration and adjusted the Specific Leaf
333 Area (SLA, m² g⁻¹) to decline with decreasing temperature using observations from Pyl *et al.*
334 2012 (Figure S7). A more accurate representation of respiration and carbon pools should be
335 incorporated into future models to improve plant growth predictions in a range of temperature
336 conditions.

337 *Plant growth conditions, RNA expression, GUS tissue analysis, and statistical analysis and*
338 *experimental controls can be found in the supplemental material.*

339

340 **Results**

341 *Behavior of CO and FT transcript accumulation in fluctuating temperatures in FM-v1.5*

342 The *FT* induction by fluctuating temperatures was incorporated through *CO* transcript, which
343 was induced in response to a change to cool temperatures like that observed (Figure 3a-b). There
344 was a strong relationship between the amount of simulated and observed *CO* transcript across
345 treatments, as calculated as the area under the curve (AUC, Figure 3c); although, FM-v1.5 does
346 not incorporate the *CO* suppression observed when plants are grown at constant 12 °C from seed
347 (12°C-constant) (Kinmonth-Schultz *et al.*, 2016). These model modifications, coupled with
348 increased *FT* transcriptional sensitivity near dawn, resulted in induction of *FT* after a temperature
349 drop at dawn or dusk like that observed (Figure 3d-e). Suppression of *FT* through SVP activity,
350 mimicked the observed *FT* suppression at dusk. When the SVP influence is removed in FM-v1.5
351 to mimic an *syp* mutant, dusk *FT* suppression in warm-day, cool-night conditions (22°C /12°C-
352 night) disappears as is observed; however, simulated morning induction of *FT* is higher, perhaps
353 because SVP activity accounts for both SVP and FLM-β (Figure S8). This strong induction

354 through *CO* was necessary in FM-v1.5 to simulate *FT* induction by cool temperatures in
355 wildtype.

356 For flowering to occur, favorable conditions must occur over several days (Kinmonth-Schultz *et*
357 *al.*, 2016; Krzymuski *et al.*, 2015; Corbesier *et al.*, 2007). Our aim was to approximate *FT*
358 behavior within a day and through time. Observed *FT* suppression at dusk in 22/12°C-night
359 conditions occurs by day two of the temperature-cycle treatment (Figure S2a). This is true with
360 FM-v1.5 as well, although *FT* levels continue to decline until day four relative to the constant-
361 temperature control (Figure S2b). Over two weeks, the increase in dusk *FT* levels in 22/12°C-
362 night conditions relative to the 22°C-constant control is similar between observed and simulated
363 data (Figure S2a-b). Together, FM-v1.5 can accommodate the wide range in *FT* transcribed
364 across treatments (Figure 2f), and *FT* behaves similarly over time to that observed, allowing us
365 to explore the temperature influence on *FT* expression and flowering in LDs.

366

367 *Assessment of FT accumulation in FM-v1.5 across temperatures*

368 FM-v1.5 allows us to assess the relative temperature influence on *FT* accumulation through both
369 gene expression and leaf development. We compared the total *FT* accumulated 9 days post
370 emergence, equivalent to 1 week in fluctuating temperature treatments, considering 1) influence
371 of temperature on gene expression only (GE), 2) *FT* accumulated with leaf tissue production as
372 influenced by thermal time, temperature influence on gene expression excluded (LTP), and 3)
373 gene expression changes incorporated with leaf tissue production (LTP+GE, full FM-v1.5
374 model). The influence of age on a leaf's capacity to express *FT* is incorporated into both the LTP
375 and LTP+GE model variants.

376 When considering LTP+GE, total *FT* declined, relative to the 22°C-constant control, with
377 increasing exposure times to cool temperature as would be expected from leaf area changes
378 (Figure 4a). When only transcriptional changes were considered (GE), *FT* accumulated at a
379 faster rate than the control for some treatments (i.e. a drop in daytime temperature, Figure 4b).
380 For treatments in which *FT* accumulated more slowly than the control, as in 12°C-constant, the
381 relative difference from the control was less extreme than in LTP+GE. For comparison, we
382 explored the relative difference in accumulated MPTUs, which control flowering time in FM-

383 v1.0, over this timeframe. MPTUs across treatments differed to a lesser degree than accumulated
384 *FT* transcript in LTP+GE, even when nighttime temperatures carried the same weight as daytime
385 temperatures (Figure 4a).

386 To assess the influence *FT* transcriptional changes due to temperature have on whole-plant *FT*
387 levels, we used the LTP model variant, meaning that temperature influenced *FT* only through
388 leaf production modulated by thermal time. LTP did differ in whole-plant accumulation. Total
389 *FT* accumulation in the warm-day, cool-night temperature cycle treatments moved closer to that
390 of the control compared to LTP+GE (Figure 4a). When the daytime temperature dropped from
391 22 °C to 12 °C (22/12°C-day) *FT* accumulated more quickly in LTP+GE than in LTP.

392 *Assessing capacity of FM-v1.5 to predict flowering*

393 How well can *FT* accumulation predict flowering? What impacts do transcriptional changes have
394 compared to that of whole-plant *FT* accumulation? To assess this, we simulated experiments for
395 plants grown in warm-day, cool-night temperature cycles (Kinmonth-Schultz *et al.*, 2016) as
396 plants often experience such temperature fluctuations in nature. We first assumed that *FT*
397 accumulates to a threshold in a manner like thermal time accumulation. This assumption is
398 consistent with observations that *FT* induction must occur over a period of days before flowering
399 is induced (Corbesier *et al.*, 2007; Krzymuski *et al.*, 2015; Kinmonth-Schultz *et al.*, 2016). We
400 set the threshold as the value of *FT* accumulated when plants reached 15 and 8 leaves, which was
401 the nearest whole number to the average leaf number at bolt for Columbia-0 (Col-0) and
402 Landsburg *erecta* (*Ler*), respectively, grown in LD 22°C-constant conditions (Kinmonth-Schultz
403 *et al.*, 2016). We maintained the strain-specific parameters for rate of emergence and leaf
404 initiation from FM-v1.0, as they were comparable to our results (Figure 5a), but added a 7-d
405 delay after initiation of the final leaf to improve the fit across strains at 22 °C. This was to
406 account for the time between initiation of the leaf primordia as modeled (Christophe *et al.*, 2008)
407 and growth of a visible bolt, counted when the stem below the bolt head was 2 mm in length
408 (Kinmonth-Schultz *et al.*, 2016).

409 We then compared the predicted final leaf number and days to bolt for warm-day, cool-night
410 temperature-cycle treatments in the LTP and LTP+GE model variants in FM-v1.5. Cool
411 temperatures delay bolting and increase leaf number (Blazquez *et al.*, 2003, Kinmonth-Schultz *et*
412 *al.*, 2016). In LTP, we expected that cool-nighttime temperatures would cause flowering to occur

413 at a similar leaf number to the 22°C-constant control because temperature was not influencing
414 gene expression; however, plants would still flower later due to slower whole-plant *FT*
415 accumulation through slower leaf growth. LTP predicted a trend opposite that observed, with a
416 lower leaf number for both 22/17°C-night and 22/12°C-night treatments (Table 1, Figure 5b),
417 because leaves that are present continue to produce *FT* such that it accumulates over time as well
418 as with leaf growth. This caused *FT* to reach the threshold at a lower leaf number. As expected,
419 both 22/17°C-night and 22/12°C-night treatments bolted later than the 22°C-constant control
420 (Table 1). The full LTP+GE variant followed a trend close to that observed, increasing the final
421 leaf number for both cool-night temperature treatments and causing a stronger delay in days to
422 bolt than LTP (Table 1, Figure 5a-c).

423 We compared this behavior to flowering predicted using MPTU accumulation by FM-v1.0,
424 adjusting the MPTU threshold to our LD 22°C-constant conditions, as recommended (Chew *et*
425 *al.*, 2014). If FM-v1.0 adequately captured temperature influence, then the MPTU threshold
426 should be similar across treatments, with negligible differences between predicted and observed
427 results for all three temperature regimes. FM-v1.0 predicted fewer leaves in both 22/12°C-night
428 and 22/17°C-night conditions than in the 22°C-constant control, because it reached the MPTU
429 target before reaching the observed final leaf number (Table 1, Figure 5b). FM-v1.0 accurately
430 captured days to bolt for Col-0 and *Ler* grown in 22°C-constant conditions, and showed an
431 expected delay in days to bolt for both 22/12°C-night and 22/17°C-night. However, the days to
432 bolt were lower than observed (Table 1, Figure 5d). Recalibrating to equalize the influence of
433 nighttime and daytime temperatures (daytime temperatures are given more weight in FM-v1.0
434 (Chew *et al.*, 2012)) reduced but did not eliminate these trends (Table 1-2, Figure 5e-f).
435 Therefore, incorporating mechanistic *FT* accumulation can improve model predictions in
436 fluctuating ambient temperature conditions (Table 2).

437

438 *Influence of FT accumulation in conditions causing later flowering*

439 As later produced leaves may lose the capacity to express *FT* (Figure 2), we wondered how this
440 would impact *FT* accumulation and flowering over longer developmental time periods, such as in
441 cool constant temperatures when *FT* is suppressed and *Arabidopsis* flowers at a higher leaf

442 number (Blazquez *et al.*, 2003). We grew Col-0 at 12 °C-constant or 22/12°C-day conditions (in
443 the latter treatment, plants then remained at 12°C). We observed flowering at 24 and 28 leaves,
444 respectively, and at 60 and 61 days after sowing. In the full FM-v1.5 LTP+GE variant, *FT* failed
445 to accumulate to the threshold set in 22 °C conditions (Figure 6). Simulated *FT* in the LTP
446 variant (temperature influence on *FT* gene expression removed), did reach the threshold in
447 22°C/12°C-day conditions (data not shown). *FT* attained the threshold in 12°C-constant, only
448 after influence of leaf age was removed from the LTP model as well. Therefore, whole-plant *FT*
449 accumulation, as influenced by leaf age, leaf tissue production, and transcriptional regulation of
450 *FT* by temperature may not be sufficient to predict flowering in conditions in which *FT* is
451 strongly suppressed under the assumption of a constant *FT* threshold.

452

453 *Influence of short-term temperature fluctuations on FT and flowering*

454 Although long-term exposure to cool temperatures suppressed whole-plant *FT* and delayed
455 flowering, temperature changes at dawn in LDs (22/12°C-day or 22/17°C-day) caused short-term
456 *FT* induction (Kinmonth-Schultz *et al.* 2016). As *FT* transcript must accumulate over several
457 days before flowering can occur (Krzymuski *et al.*, 2015), we wondered whether a short-term
458 temperature drop, causing *FT* induction, could complement *FT* produced in subsequent warm
459 temperatures to accelerate flowering, or if slower whole-plant *FT* accumulation with slower leaf
460 growth would delay flowering. To compare the predicted influence of *FT* induction by
461 temperature fluctuations, we used the FM-v1.5 LTP+GE and LTP variants to simulate two-week-
462 old plants moved to 12 °C in LDs for two, four, or six days (12°C-2d, -4d, or -6d), then moved to
463 warm, LD conditions. We also grew plants in these conditions. Control plants were moved
464 directly to warm, LD conditions at two weeks.

465 Simulating these conditions in the full LTP+GE variant of FM-v1.5, we found little difference in
466 days to bolt between 12°C-2d and the control and a three-day difference between 12°C-6d and
467 the control. There was a decline in leaf number from 15 to 14 leaves in plants exposed to 12°C-
468 2d and 12°C-4d, indicating flowering at a slightly younger developmental age that translated to
469 little difference in days to bolt between the control and 12°C-2d. In 12°C-6d, the leaf number
470 increased again to be like the control. In the LTP variant, the leaf number of all three treatments

471 was the same as the control, whereas there was an increase in days to bolt for each consecutive
472 two-days at 12 °C, consistent with slowed accumulation of *FT* due to slower leaf growth.

473 We observed slowed growth (relative to the control) in the cool-temperature treatments. Visible
474 leaf number was significantly lower after four and six days in 12 °C (Figure 7a). On day seven,
475 after completion of all cool-temperature treatments, there was a gradient in leaf area across
476 treatments, with plants from 12°C-6d being the smallest (Figure 7b, S8). We observed a
477 statistically significant delay in the number of days to visible bolt in both 12°C-4d and 12°C-6d,
478 like both simulations ($P < 0.001$, Table 3, Figure 7c). While we did not observe a significant
479 difference in leaf number in either 12°C-2d or 12°C-4d relative to the control, plants in 12°C-6d
480 produced approximately 1.5 more leaves before flowering than the other three treatments
481 ($P < 0.001$), more like the predicted increase in leaf number from 12°C-2d and 12°C-4d to 12°C-
482 6d in the LTP+GE model variant (Table 3).

483 Discussion

484 Incorporating underlying mechanisms could improve model utility for a range of conditions
485 without requiring recalibration (White, 2009; Boote *et al.*, 2013). Here, we found that thermal
486 time (MPTUs) did predict delays in days to bolt under fluctuating temperature conditions in LDs
487 relative to the constant-temperature control, but the delays were less than observed and more like
488 FM-v1.5 LTP, in which *FT* accumulated only with leaf growth, a function of thermal time (Table
489 1, Figure 5b & d). Adding direct temperature regulation of *FT* improved model predictions by
490 increasing the degree of predicted difference between the warm-day, cool-night treatments and
491 the control.

492 *FT* was reduced in later-produced leaves (Figure 2). This change in *FT* expression with
493 developmental age was incorporated into FM-v1.5 using leaf age as a proxy, and caused *FT* to
494 fail to accumulate to a preset threshold to predict flowering in constant cool temperatures. This
495 finding enables integration of qualitative (presence/absence) and quantitative (dosage response)
496 aspects of *FT* effects on flowering, and has implications for other conditions in which *FT* is
497 suppressed, such as in short daylengths. It can help us quantify when *FT* plays a role during
498 development, when *FT* alone is a poor predictor of flowering, and when it may act
499 synergistically or competitively with other flowering factors.

500 For instance, the *FT* threshold requirement should be influenced by shoot-apex genes; their
501 sensitivity likely changes with climate and developmental age. For example, in short-days, high
502 temperatures may reduce SVP activity at the shoot apex to initiate flowering despite lower *FT*
503 levels (Fernández *et al.*, 2016). At the shoot apex, SVP suppresses *SUPPRESSOR OF*
504 *OVEREXPRESSION OF CONSTANS (SOC1)*, which is positively regulated by *FT*, and which
505 activates *LEAFY (LFY)*, a key player in the floral transition (Schmid *et al.*, 2003; Lee *et al.*,
506 2008; Jang *et al.*, 2009). *FT* protein also activates *APETALA1 (API)* at the shoot apex (Lee &
507 Lee, 2010). *API*, in turn, is involved in the down regulation of *TERMINAL FLOWERING1*
508 (*TFL1*), a *FT* homolog. *TFL1* is thought to compete with *FT* for binding with *FD* to suppress
509 *LFY*, as well as *API*, forming a negative feedback loop (Kaufmann *et al.*, 2010; Wickland &
510 Hanzawa, 2015). Both the decrease in SVP and *TFL1* would likely decrease the *FT* threshold
511 needed to induce flowering. Like *SVP*, *TFL1* may be temperature sensitive (Kim *et al.*, 2013).

512 A changing threshold, due to different *LATE FLOWERING* alleles in *Pea*, a homologue of *TFL1*
513 in *Arabidopsis* (Foucher *et al.*, 2003), aids flowering time predictions (Wenden *et al.*, 2009).
514 Incorporating such a mechanism – influenced by climate and developmental age – may aid
515 understanding of how climate influences flowering. As proof of concept, we caused the *FT*
516 threshold level to change with developmental age (thermal time) (Figure 6). Doing so improved
517 the predictive capacity of FM-v1.5 in constant, cool temperatures.

518 *SVP*, in conjunction with *FLM*, suppresses *FT* in response to cool temperatures (Blazquez *et al.*,
519 2003; Lee *et al.*, 2007, 2013). We demonstrated that residual *SVP* and *FLM* activity after short-
520 term cold exposures could be important for *FT* regulation. For instance, to mimic observed dusk
521 suppression of *FT* in warm-day, cool-night temperature cycles, simulated *SVP* activity decayed
522 slowly after at 12 °C night, such that it was higher after 16 hs at 22 °C, than it was in constant 22
523 °C conditions. Our model also highlights the need to clarify the degree of temperature influence
524 in *FT* activation and suppression at a range of temperatures. For example, in FM-v1.5, *FT* is not
525 induced to observed levels, and induction is not maintained as long, after dawn exposure to 17 °C
526 (Figure 3f). It is possible that *SVP* activation is lower in 17 °C, than predicted from our model.
527 However, the relative difference in transcript levels across treatments is similar to the relative
528 difference in daytime *FT* expression, which correlates most strongly with flowering (Krzymuski
529 *et al.*, 2015; Kinmonth-Schultz *et al.*, 2016).

530 Our simulations, while requiring validation in other temperature conditions, are consistent with
531 approaches that use day length and vernalization to influence the leaf number at which the
532 reproductive transition occurs (Brown *et al.*, 2013). However, our work demonstrates that
533 ambient temperature should be incorporated to influence leaf number as well, not only
534 developmental rate. For instance, we altered *FT* accumulation, either by removing temperature
535 influence on *FT* transcription (FM-v1.5 LTP, Table 2) or by short-term, cool-temperature
536 exposure (Figure 3d-e, Table 3), affecting final leaf number. In each instance, *FT* still
537 accumulated with leaf production as influenced by temperature, demonstrating that temperature
538 influences when (in days) the reproductive transition occurs by influencing the developmental
539 rate and whole-plant *FT* accumulation. We further suggest that tissue accumulation through
540 growth is an underlying factor in the accumulation of thermal time as it causes gene products to
541 accumulate. Together, this work demonstrates that decomposing the influences of climate and
542 development can improve our understanding of plant responses in a range of conditions.

543

544 **Supplementary Data**

545 **Section S1:** Materials and Methods for plant growth conditions, RNA expression, GUS tissue
546 analysis, and statistical analysis and experimental controls.

547 **Section S2:** Equation used in FM-v1.0 to describe *FT* transcription as a function of CO protein.

548 **Table S1:** Coefficients values for equations used in FM-v1.5.

549 **Figure S1.** Graphic representation of FM-V1.

550 **Figure S2.** SVP/FLM activity declines over time.

551 **Figure S3.** Behavior of *CO* mRNA in response to different temperature regimes.

552 **Figure S4.** Simulated expression profile of *LHY*, plotted over time used to increase morning
553 transcriptional sensitivity of *FT*.

554 **Figure S5.** The spatial expression profile of *FT* changes with leaf age.

555 **Figure S6:** Behavior of morphological and physiological parameters in FM-v1.0 and v1.5.

556 **Figure S7.** Original photograph used for Figure 7 showing Specific Leaf Area (SLA) declines after
557 growth in cool constant temperatures or in warm-day, cool-night temperature cycles relative to a constant,
558 warm-temperature control.

559 **Figure S8.** Simulated *FT* expression profile in FM-v1.5 in the *syp* mutant mimics the pattern but not
560 relative amplitude of that observed.

561

562 **Acknowledgements**

563 Many thanks the Jennifer Nemhauser lab for use of their dissecting scope and to Paul Panipinto
564 for help on this project. This work was supported in part by a Cooperative Research Program for
565 Agricultural Science and Technology Development (PJ0127872017), Rural Development
566 Administration, Republic of Korea and a Specific Cooperative Agreement (58-8042-6-097)
567 between University of Washington and USDA-ARS to S.-H.K; by National Institute of Health
568 grant (GM079712), Next-Generation BioGreen 21 Program (SSAC, PJ011175, Rural
569 Development Administration, Republic of Korea) to T.I.; by a Biotechnology and Biological
570 Sciences Research Council awards (BB/L026996, BB/N012348) to A.J.M.; and by the
571 University of Washington Biology Department Frye-Hotson-Rigg Fellowship to H.K.S.

References

Abe M, Kobayashi Y, Yamamoto S, Daimon Y, Yamaguchi A, Ikeda Y, Ichinoki H, Notaguchi M, Goto K, Araki T. 2005. FD, a bZIP protein mediating signals from the floral pathway integrator FT at the shoot apex. *Science* **309**: 1052–6.

Amasino R. 2010. Seasonal and developmental timing of flowering. *Plant Journal* **61**: 1001–1013.

Asseng S, Ewert F, Rosenzweig C, Jones JW, Hatfield JL, Ruane AC, Boote KJ, Thorburn PJ, Rötter RP, Cammarano D, et al. 2013. Uncertainty in simulating wheat yields under climate change. *Nature Climate Change* **3**: 827–832.

Blazquez M, Ahn J, Weigel D. 2003. A thermosensory pathway controlling flowering time in *Arabidopsis thaliana*. *Nature Genetics* **33**: 168–171.

Boote KJ, Jones JW, White JW, Asseng S, Lizaso JI. 2013. Putting mechanisms into crop production models. *Plant, Cell and Environment* **36**: 1658–1672.

Bratzel F, Turck F. 2015. Molecular memories in the regulation of seasonal flowering: from competence to cessation. *Genome Biology* **16**: 192–206.

Brown HE, Jamieson PD, Brooking IR, Moot DJ, Huth NI. 2013. Integration of molecular and physiological models to explain time of anthesis in wheat. *Annals of Botany* **112**: 1683–1703.

Carter JM, Orive ME, Gerhart LM, Stern JH, Marchin RM, Nagel J, Ward JK. 2017. Warmest extreme year in U.S. history alters thermal requirements for tree phenology. *Oecologia* **183**: 1197–1210.

Chew YH, Wenden B, Flis A, Mengin V, Taylor J, Davey CL, Tindal C, Thomas H, Ougham HJ, Reffye P de, et al. 2014. Multiscale digital *Arabidopsis* predicts individual organ and whole-organism growth. *Proceedings of the National Academy of Sciences* **111**: E4127–E4136.

Chew YH, Wilczek AM, Williams M, Welch SM, Schmitt J, Halliday KJ. 2012. An augmented *Arabidopsis* phenology model reveals seasonal temperature control of flowering time. *New Phytologist* **194**: 654–665.

Christophe A, Letort V, Hummel I, Cournède P-H, Reffye P de, Lecœur J. 2008. A model-based analysis of the dynamics of carbon balance at the whole-plant level in *Arabidopsis thaliana*. *Functional Plant Biology* **35**: 1147–1162.

Chuine I. 2000. A unified model for budburst of trees. *Journal of Theoretical Biology* **207**: 337–347.

Corbesier L, Vincent C, Jang S, Fornara F, Fan Q, Searle I, Giakountis A, Farrona S, Gissot L, Turnbull C, et al. 2007. FT protein movement contributes to long-distance signaling in floral induction of *Arabidopsis thaliana*. *Science* **316**: 1030–1033.

Fernández V, Takahashi Y, LeGourrierc J, Coupland G. 2016. Photoperiodic and thermosensory pathways interact through CONSTANS to promote flowering at high temperature under short days. *Plant Journal* **86**: 426–440.

- Foucher F, Morin J, Courtiade J, Cadioux S, Ellis N, Banfield MJ, Rameau C. 2003.** *DETERMINATE* and *LATE FLOWERING* are two *TERMINAL FLOWER1/CENTRORADIALIS* homologs that control two distinct phases of flowering initiation and development in pea. *Plant Cell* **15**: 2742–2754.
- Franklin KA, Whitelam GC. 2007.** Light-quality regulation of freezing tolerance in *Arabidopsis thaliana*. *Nat Genet* **39**: 1410–1413.
- He J, Le Gouis J, Stratonovitch P, Allard V, Gaju O, Heumez E, Orford S, Griffiths S, Snape JW, Foulkes MJ, et al. 2012.** Simulation of environmental and genotypic variations of final leaf number and anthesis date for wheat. *European Journal of Agronomy* **42**: 22–33.
- Heinsvig Kjær K, Thorup-Kristensen K, Rosenqvist E, Mazanti Aaslyng J. 2007.** Low night temperatures change whole-plant physiology and increase starch accumulation in *Chrysanthemum morifolium*. *Journal of Horticultural Science & Biotechnology* **82**: 867–874.
- Helliwell CA, Wood CC, Robertson M, James Peacock W, Dennis ES. 2006.** The *Arabidopsis thaliana* FLC protein interacts directly in vivo with *SOC1* and *FT* chromatin and is part of a high-molecular-weight protein complex. *Plant Journal* **46**: 183–192.
- Jaglo-Ottosen KR, Gilmour SJ, Zarka DG, Schabenberger O, Thomashow MF. 1998.** *Arabidopsis CBF1* overexpression induces *COR* genes and enhances freezing tolerance. *Science* **280**: 104–106.
- Jamieson PD, Brooking IR, Semenov MA, Porter JR. 1998a.** Making sense of wheat development: a critique of methodology. *Field Crops Research* **55**: 117–127.
- Jamieson PD, Semenov MA, Brooking IR, Francis GS. 1998b.** Sirius: a mechanistic model of wheat response to environmental variation. *European Journal of Agronomy* **8**: 161–179.
- Jang S, Torti S, Coupland G. 2009.** Genetic and spatial interactions between *FT*, *TSF* and *SVP* during the early stages of floral induction in *Arabidopsis*. *Plant Journal* **60**: 614–625.
- Jones JW, Hoogenboom G, Porter CH, Boote KJ, Batchelor WD, Hunt LA, Wilkens PW, Singh U, Gijsman AJ, Ritchie JT. 2003.** The DSSAT cropping system model. *European Journal of Agronomy* **18**: 235–265.
- Karsai I, Igartua E, Casas AM, Kiss T, Soos V, Balla K, Bedo Z, Veisz O. 2013.** Developmental patterns of a large set of barley (*Hordeum vulgare*) cultivars in response to ambient temperature. *Annals of Applied Biology* **162**: 309–323.
- Karsai I, Szucs P, Koszegi B, Hayes PM, Casas A, Bedo Z, Veisz O. 2008.** Effects of photo and thermo cycles on flowering time in barley: a genetical phenomics approach. *Journal of Experimental Botany* **59**: 2707–2715.
- Kaufmann K, Wellmer F, Muiño JM, Ferrier T, Wuest SE, Kumar V, Serrano-Mislata A, Madueño F, Krajewski P, Meyerowitz EM, et al. 2010.** Orchestration of floral initiation by APETALA1. *Science* **328**: 85–89.
- Kim S-H, Gitz DC, Sicher RC, Baker JT, Timlin DJ, Reddy VR. 2007.** Temperature dependence of growth, development, and photosynthesis in maize under elevated CO₂. *Environmental and Experimental Botany* **61**: 224–236.

Kim W, Park TI, Yoo SJ, Jun AR, Ahn JH. 2013. Generation and analysis of a complete mutant set for the *Arabidopsis* *FT/TFL1* family shows specific effects on thermo-sensitive flowering regulation. *Journal of Experimental Botany* **64**: 1715–1729.

Kim S-H, Yang Y, Timlin DJ, Fleisher DH, Dathe A, Reddy VR, Staver K. 2012. Modeling temperature responses of leaf growth, development, and biomass in maize with MAZSIM. *Agronomy Journal* **104**: 1523–1537.

Kinmonth-Schultz HA, Tong X, Lee J, Song YH, Ito S, Kim S-H, Imaizumi T. 2016. Cool night-time temperatures induce the expression of *CONSTANS* and *FLOWERING LOCUS T* to regulate flowering in *Arabidopsis*. *New Phytologist* **211**: 208–224.

Krzymuski M, Andrés F, Cagnola JI, Seonghoe J, Yanovsky M, Coupland G, Casal JJ. 2015. The dynamics of *FLOWERING LOCUS T* expression encodes long-day information. *Plant journal* **83**: 952–961.

Kumudini S, Andrade FH, Boote KJ, Brown GA, Dzotsi KA, Edmeades GO, Gocken T, Goodwin M, Halter AL, Hammer GL, et al. 2014. Predicting maize phenology: Intercomparison of functions for developmental response to temperature. *Agronomy Journal* **106**: 2087–2097.

Lee J, Lee I. 2010. Regulation and function of *SOC1*, a flowering pathway integrator. *Journal of Experimental Botany* **61**: 2247–2254.

Lee J, Oh M, Park H, Lee I. 2008. *SOC1* translocated to the nucleus by interaction with *AGL24* directly regulates *LEAFY*. *Plant Journal* **55**: 832–843.

Lee JH, Ryu H-S, Chung KS, Posé D, Kim S, Schmid M, Ahn JH. 2013. Regulation of temperature-responsive flowering by *MADS*-Box transcription factor repressors. *Science* **342**: 628–632.

Lee JH, Yoo SJ, Park SH, Hwang I, Lee JS, Ahn JH. 2007. Role of *SVP* in the control of flowering time by ambient temperature in *Arabidopsis*. *Genes & Development* **21**: 397–402.

Lehenbauer PA. 1914. Growth of maize seedlings in relation to temperature. *Physiological Researches* **1**: 247–288.

Lutz U, Posé D, Pfeifer M, Gundlach H, Hagemann J, Wang C, Weigel D, Mayer KFX, Schmid M, Schwechheimer C. 2015. Modulation of ambient temperature-dependent flowering in *Arabidopsis thaliana* by natural variation of *FLOWERING LOCUS M*. *PLoS Genetics* **11**: e1005588.

Makowski D, Asseng S, Ewert F, Bassu S, Durand JL, Li T, Martre P, Adam M, Aggarwal PK, Angulo C, et al. 2015. A statistical analysis of three ensembles of crop model responses to temperature and CO₂ concentration. *Agricultural and Forest Meteorology* **214**: 483–493.

Mathieu J, Yant LJ, Mürdter F, Küttner F, Schmid M. 2009. Repression of flowering by the miR172 target *SMZ*. *PLoS Biology* **7**: e1000148.

Parent B, Turc O, Gibon Y, Stitt M, Tardieu F. 2010. Modelling temperature-compensated physiological rates, based on the co-ordination of responses to temperature of developmental processes. *Journal of Experimental Botany* **61**: 2057–2069.

Piper EL, Smit MA, Boote KJ, Jones JW. 1996. The role of daily minimum temperature in modulating the development rate to flowering in soybean. *Field Crops Research* **47**: 211–220.

Posé D, Verhage L, Ott F, Yant L, Mathieu J, Angenent GC, Immink RGH, Schmid M. 2013. Temperature-dependent regulation of flowering by antagonistic FLM variants. *Nature* **503**: 414–417.

Pyl E-T, Piques M, Ivakov A, Schulze W, Ishihara H, Stitt M, Sulpice R. 2012. Metabolism and growth in *Arabidopsis* depend on the daytime temperature but are temperature-compensated against cool nights. *Plant Cell* **24**: 2443–2469.

Rasse DP, Tocquin P. 2006. Leaf carbohydrate controls over *Arabidopsis* growth and response to elevated CO₂: an experimentally based model. *New Phytologist* **172**: 500–513.

Rensing L, Ruoff P. 2002. Temperature effect on entrainment, phase shifting, and amplitude of circadian clocks and its molecular bases. *Chronobiology International* **19**: 807–864.

Ritchie J, Otter S. 1985. Description and performance of CERES-Wheat. A user-oriented wheat model. *US Department of Agriculture, ARS* **38**: 159–175.

Salazar JD, Saithong T, Brown PE, Foreman J, Locke JCW, Halliday KJ, Carré IA, Rand DA, Millar AJ. 2009. Prediction of photoperiodic regulators from quantitative gene circuit models. *Cell* **139**: 1170–1179.

Schmid M, Uhlenhaut NH, Godard F, Demar M, Bressan R, Weigel D, Lohmann JU. 2003. Dissection of floral induction pathways using global expression analysis. *Development* **130**: 6001–6012.

Schwartz C, Balasubramanian S, Warthmann N, Michael TP, Lempe J, Sureshkumar S, Kobayashi Y, Maloof JN, Borevitz JO, Chory J, et al. 2009. Cis-regulatory changes at *FLOWERING LOCUS T* mediate natural variation in flowering responses of *Arabidopsis thaliana*. *Genetics* **183**: 723–732.

Searle I, He Y, Turck F, Vincent C, Fornara F, Kröber S, Amasino RA, Coupland G. 2006. The transcription factor FLC confers a flowering response to vernalization by repressing meristem competence and systemic signaling in *Arabidopsis*. *Genes & Development* **20**: 898–912.

Seaton DD, Smith RW, Song YH, MacGregor DR, Stewart K, Steel G, Foreman J, Penfield S, Imaizumi T, Millar AJ, et al. 2015. Linked circadian outputs control elongation growth and flowering in response to photoperiod and temperature. *Molecular Systems Biology* **11**: 1–19.

Segal IH. 1976. *Biochemical Calculations: How to Solve Mathematical Problems in General Biochemistry*. Canada: John Wiley and Sons.

Song Y-H, Shim J-S, Kinmonth-Schultz HA, Imaizumi T. 2015. Photoperiodic flowering: time measurement mechanisms in leaves. *Annual Review of Plant Biology* **66**: 441–464.

Sperling O, Earles JM, Secchi F, Godfrey J, Zwieniecki MA. 2015. Frost induces respiration and accelerates carbon depletion in trees. *Plos One* **10**: e0144124.

- Sureshkumar S, Dent C, Seleznev A, Tasset C, Balasubramanian S. 2016.** Nonsense-mediated mRNA decay modulates FLM-dependent thermosensory flowering response in *Arabidopsis*. *Nature Plants* **2**: 16055.
- Takada S, Goto K. 2003.** TERMINAL FLOWER2, an Arabidopsis homolog of HETEROCHROMATIN PROTEIN1, counteracts the activation of *FLOWERING LOCUS T* by CONSTANS in the vascular tissues of leaves to regulate flowering time. *Plant Cell* **15**: 2856–2865.
- Thines BC, Youn Y, Duarte MI, Harmon FG. 2014.** The time of day effects of warm temperature on flowering time involve PIF4 and PIF5. *Journal of Experimental Botany* **65**: 1141–1151.
- Welch SM, Roe JL, Dong Z. 2003.** A genetic neural network model of flowering time control in *Arabidopsis thaliana*. *Agronomy Journal* **95**: 71–81.
- Wenden B, Dun EA, Hanan J, Andrieu B, Weller JL, Beveridge CA, Rameau C. 2009.** Computational analysis of flowering in pea (*Pisum sativum*). *New Phytologist* **184**: 153–167.
- White JW. 2009.** Combining ecophysiological models and genomics to decipher the GEM-to-P problem. *NJAS - Wageningen Journal of Life Sciences* **57**: 53–58.
- Wickland DP, Hanzawa Y. 2015.** The *FLOWERING LOCUS T*/*TERMINAL FLOWER 1* gene family: functional evolution and molecular mechanisms. *Molecular Plant* **8**: 983–997.
- Wilczek AM, Roe JL, Knapp MC, Cooper MD, Lopez-Gallego C, Martin LJ, Muir CD, Sim S, Walker A, Anderson J, et al. 2009.** Effects of genetic perturbation on seasonal life history plasticity. *Science* **323**: 930–934.
- Yan L, Fu D, Li C, Blechl A, Tranquilli G, Bonafede M, Sanchez A, Valarik M, Yasuda S, Dubcovsky J. 2006.** The wheat and barley vernalization gene *VRN3* is an orthologue of *FT*. *Proceedings of the National Academy of Sciences* **103**: 19581–19586.
- Yin X, Kropff M. 1996.** The effect of temperature on leaf appearance in rice. *Annals of Botany* **77**: 215–221.
- Yin X, Kropff MJ, McLaren G, Visperas RM. 1995.** A nonlinear model for crop development as a function of temperature. *Agricultural and Forest Meteorology* **77**: 1–16.
- Zheng B, Biddulph B, Li D, Kuchel H, Chapman S. 2013.** Quantification of the effects of *VRN1* and *Ppd-D1* to predict spring wheat (*Triticum aestivum*) heading time across diverse environments. *Journal of Experimental Botany* **64**: 3747–3761.

Tables

Table 1: Observed and simulated days to bolt and leaf number in Columbia-0 (Col-0) and Landsberg *erecta* (Ler) plants exposed to short-term drops in temperature.

Strain		Treatment	Obs. data	FM-v1.0	FM-v1.5 LTP+GE	FM-v1.5 LTP
Col-0	Days to bolt	22 °C day 22 °C night	32.27	30.33	35.00	35.00
		22 °C day 17 °C night	38.60	30.63	38.50	35.96
		22 °C day 12 °C night	40.08	31.25	44.88	37.50
	Leaf number	22 °C day 22 °C night	14.77	18.00	15.00	15.00
		22 °C day 17 °C night	20.50	16.00	17.00	13.00
		22 °C day 12 °C night	20.79	14.00	22.00	13.00
Ler	Days to bolt	22 °C day 22 °C night	27.13	27.75	25.42	25.42
		22 °C day 17 °C night	32.75	28.29	26.50	25.67
		22 °C day 12 °C night	33.23	28.63	29.33	25.79
	Leaf number	22 °C day 22 °C night	7.40	14.00	8.00	8.00
		22 °C day 17 °C night	8.17	13.00	8.00	7.00
		22 °C day 12 °C night	9.98	12.00	9.00	7.00

Table 2: Fit of FM-v1.0 and FM-v1.5 for Columbia-0 and Landsberg *erecta* combined.

		FM-v1.0	FM-v1.0 (Night = Day)	FM-v1.5 LTP+GE
Days to Bolt	RMSE	5.65	3.69	3.95
	Bias	-4.30	-2.69	0.11
Leaf Number	RMSE	5.56	4.91	2.67
	Bias	0.79	2.33	-0.07

Table 3: Observed and simulated days to bolt and leaf number of rosette leaves on the main stem in Columbia plants exposed to short-term drops 12 °C temperature relative to plants remaining in the warm temperature control (24 °C) in long days (LD).

	treatment	Obs. Data	n	Robust S.E.	Robust z	P -Value	C.I. of dif. (lower)	C.I. of dif. (upper)	FM-v1.5 LTP+GE	FM-v1.5 LTP
Days to bolt	LD24C (int)	35.00	11	0.62	31.10				34.75	34.75
	12C, 2d	36.00	15	0.60	1.73	0.08	-0.65	2.73	34.92	35.75
	12C, 4d	37.31	14	0.42	5.54	0.00	0.87	3.80	35.83	36.62
	12C, 6d	38.64	14	0.35	7.85	0.00	2.24	5.02	37.79	37.58
Leaf number	LD24C (int)	13.73	11	0.52	19.59				15.00	15.00
	12C, 2d	13.13	15	0.34	-1.21	0.23	-0.81	1.65	14.00	15.00
	12C, 4d	13.64	14	0.36	0.49	0.63	-1.07	1.42	14.00	15.00
	12C, 6d	15.14	14	0.39	3.47	0.00	0.08	2.64	15.00	15.00

Observed treatments counted significantly different from the control when $P < 0.05$ and the confidence interval of the difference from the control does not contain zero.

Figure Legends

Figure 1. Schematic of Model FM-v1.5. Temperature (through *CONSTANS* and *SHORT VEGETATIVE GROWTH/FLOWERING LOCUS M*), day length, and the circadian clock regulate expression of *FLOWERING LOCUS T (FT)* in the Photoperiodism and Phenology modules per unit tissue. The leaf number and relative leaf age, outputs of the Functional Structural Plant module, are used to determine the capacity of each leaf to express *FT*, and leaf area is used to determine the amount of leaf tissue present. *FT* is summed across all leaves in a plant and added to the whole-plant *FT* from the previous time step. The model ceases leaf production and determines the days to bolt (DtB) when *FT* reaches a pre-set threshold set by using the leaf number for plants grown in long days at 22 °C. Red illustrates where adjustments were made to the original model (FM-v1.0). The bold, italic numerals correspond to the numbers in the model description in the main text.

Figure 2. *FT* expression declines in later produced leaves. Leaves of plants aged two (**a**), four (**b**), and six (**c**) weeks old and grown in short days were exposed to long days or short days (**d**) for three days, then harvested at 16 hours after dawn on the third day to determine *FT* amount per leaf. The colors in (**d**) correspond to the colors and ages in panels (**a-c**). *FT* levels were determined by absolute copy number and normalized within a replicate. The simulated proportion of *FT* per unit leaf tissue (cm⁻², solid lines) for each plant age is shown. This value was used in FM-v1.5 as a modifier to adjust the amount of *FT* produced by each leaf. Percent of the leaf area showing staining in *pFT:GUS* plants (**e**). For all, the two cotyledons and first two true leaves were pooled for each sample as they emerge in pairs. Older leaves in the six-week old plants failed to yield 2µg total RNA and were excluded. For each plant inset, asterisk indicates one of each cotyledon pair. The shading of the bar graphs (light to dark) indicates leaf age (oldest, first to emerge, to youngest) and corresponds to the shading in the plant insets. Scale bars = 0.5 cm.

Figure 3. FM-v1.5 mimics general behaviors of *CO* and *FT* in response to temperature, and can accommodate the overall change in amount across treatments. Observed (**a, d**) and predicted (**b, e**) diurnal patterns of *CO* (**a, b**) and *FT* (**d, e**) gene expression in warm (22 °C)-day, cool (12 °C)-night temperature-cycle treatments and in conditions in which the temperature dropped from 22 °C to 12 °C at dawn, then remained at the cooler temperature (22 to 12 °C day) relative to the 22 °C-constant temperature control. The y-axis (**a, b, d, e**) is in zeitgeber time (ZT), and represents hours after dawn. The white and black bars represent light and dark periods respectively. Error bars = 1 S. E. If error bars are not visible, the S. E. is smaller than the height of the symbol. Correlation between predicted and observed results for *CO* (**c**) and *FT* (**f**), as calculated as the area under the curve (AUC) four days after temperature treatments are imposed. Treatments include warm-day, cool-night cycles, drops to cooler temperatures at dawn, and growth from seed at constant temperatures. All treatment groups include 12, 17 and 22 °C. Dotted lines = correlation, solid lines = one-to-one line. Open circles are growth from seed at 12 °C (**c**) and drop from 22 °C to 17 °C at dawn (**f**).

Figure 4. (**a, b**) Whole-plant *FT* accumulation influenced by temperature in fluctuating and constant-cool temperature conditions, differs more strongly from the 22 °C control than does accumulated Modified Photothermal Units (MPTUs). Total *FT* accumulated in constant and fluctuating temperature conditions relative to 22 °C constant temperatures (indicated by arrowheads) 9 ds post emergence, equivalent to 1 wk in fluctuating temperature treatments. (**a**)

LTP+GE: *FT* accumulation in full FM-v1.5 model, i.e. temperature affects *FT* gene expression through *CO* and *SVP/FLM* as well as through leaf tissue production; **LTP:** *FT* accumulation only with leaf tissue production as influenced by thermal time, temperature influence on *FT* gene expression excluded; **MPTU:** Accumulated Modified Photothermal Units from FM-v1.0. Here, daytime and nighttime temperatures are given equal weight. **(b) GE:** *FT* accumulation considering only influence of temperature on *FT* gene expression, decoupled from leaf production. 22 °C day 12 or 17 °C night indicates warm-day, cool, night cycles, 22 to 12 or 17 °C day indicates treatments in which the temperature drop occurred at dawn, then remained cool for the duration of the experiment, *constant* indicates temperatures remained constant from seed.

Figure 5: *FT* accumulation as influenced through *CO* and *SVP/FLM* and leaf tissue production can improve model predictions in fluctuating temperature conditions compared to Modified Photothermal Units (MPTUs). **(a)** Comparison of simulated (lines. FM-v1.5 LTP+GE) and observed (symbols) leaf number by week in Col in constant 22 °C conditions and in 22 °C-day, 12°C-night temperature cycles. **(b)** Final leaf number of Columbia-0 (Col) at bolt as observed (obs.) and predicted (pred.) by incorporating temperature influence on *FT* through leaf tissue production (LTP) and *FT* gene expression (GE) (FM-v1.5 LTP+GE), leaf tissue production only (FM-v1.5 LTP), and through traditional Modified Photothermal Units (MPTU) in FM-v1.0. **(c, d)** The difference between predicted and observed days to bolt in Columbia-0 (Col) and Landsberg *erecta* (Ler) using FM-v1.5 LTP+GE **(c)** and MPTUs in FM-v1.0 **(d)**. **(e)** Observed and predicted final leaf number and **(f)** the difference between predicted and observed results using MPTUs in FM-v1.0, adjusted so that daytime and nighttime temperatures are given equal weight. **(b-f)** Plotted over three nighttime temperatures. Daytime temperature was 22 °C. **(c, d, f)** Horizontal line at zero is the position in which there is no difference between predicted and observed results. Error bars = 1 S. D. If error bars are not visible, the S. D. is smaller than the height of the symbol.

Figure 6: Plants grown at constant cool (12 °C) temperatures from seed (constant) or after one week at 22 °C (22 to 12 °C day) do not accumulate *FT* to a threshold set using 22 °C constant temperatures in long days (thick black line). Altering the threshold to decline with developmental time (thick gray line) improves the predictive capacity of FM-v1.5.

Figure 7: Growth is slowed and flowering is delayed in plants exposed to 12 °C for two, four, or six days, then returned to warm temperatures (24 °C), relative to control plants grown continuously in warm-temperatures. **(a)** Average leaf number of plants recorded at dawn after two, four, or six days in 24 °C (control) or 12 °C temperature conditions. **(b)** Relative seedling sizes on dawn of day seven, after completion of all cool-temperature treatments (scale bars = 1cm, 0 = control). Individual images cropped from the same photograph and scaled together (see original image, Figure S9). **(c)** Relative flowering progression three days after appearance of last floral stem (bolt) in plants exposed to 12 °C for two, four, or six days relative to 24 °C control (0, scale bar = 5cm).

Figure 1

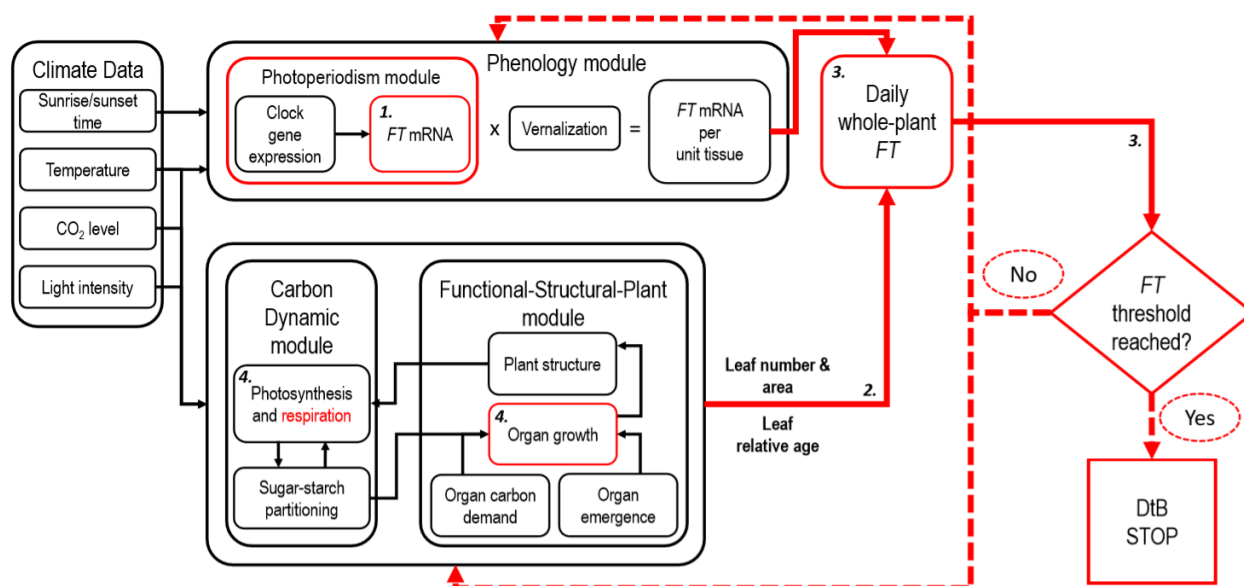


Figure 2

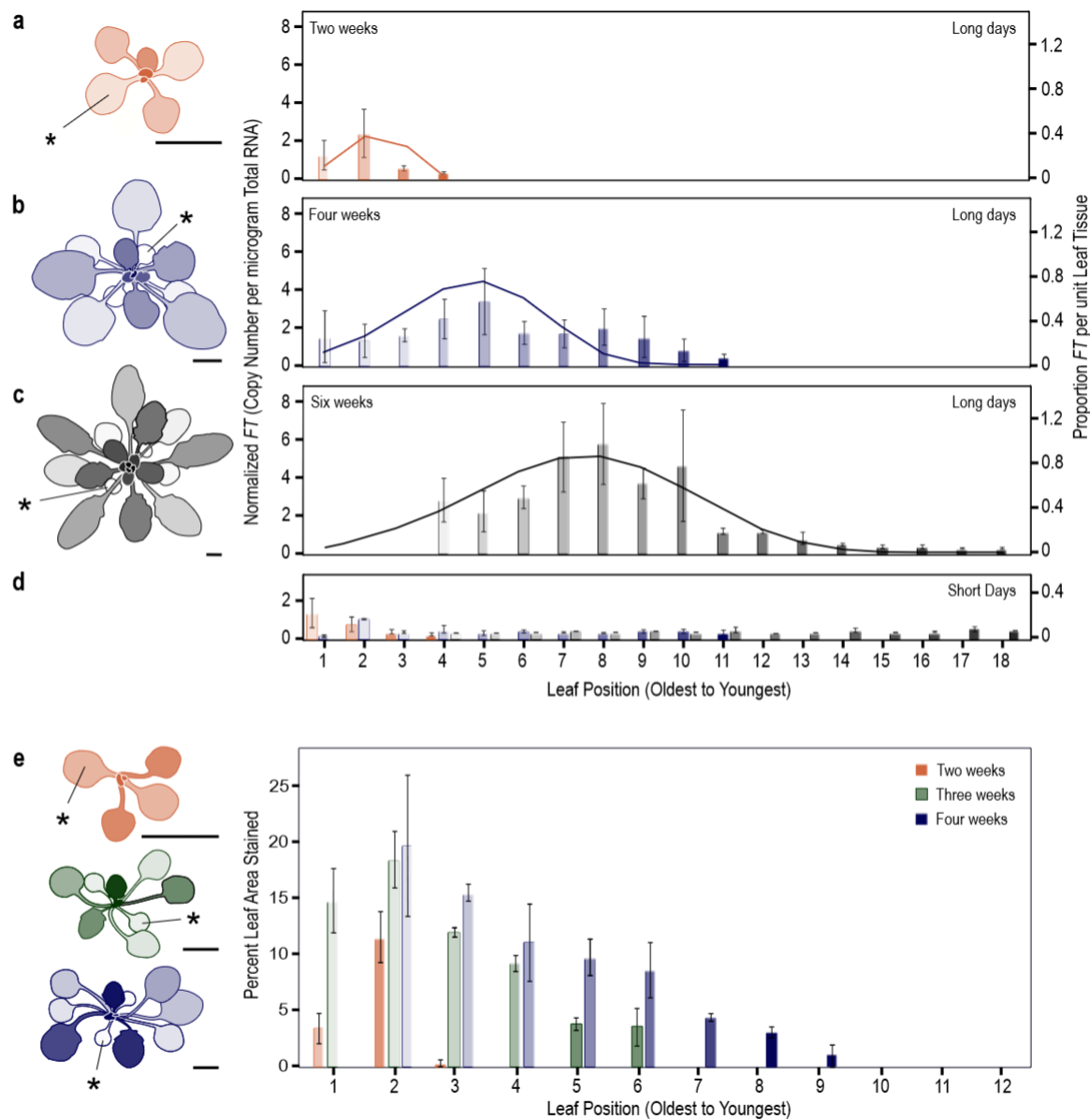


Figure 3

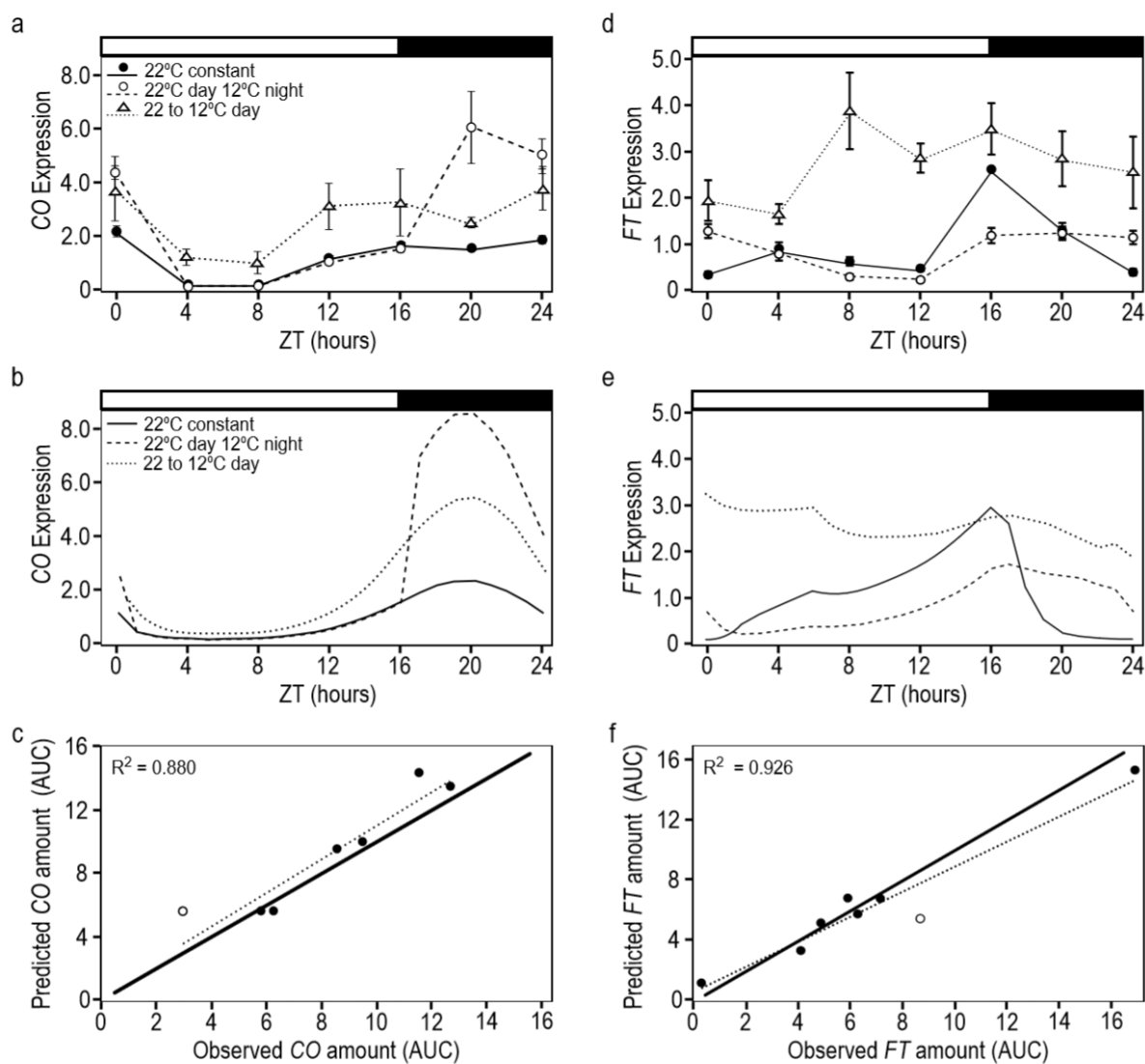


Figure 4

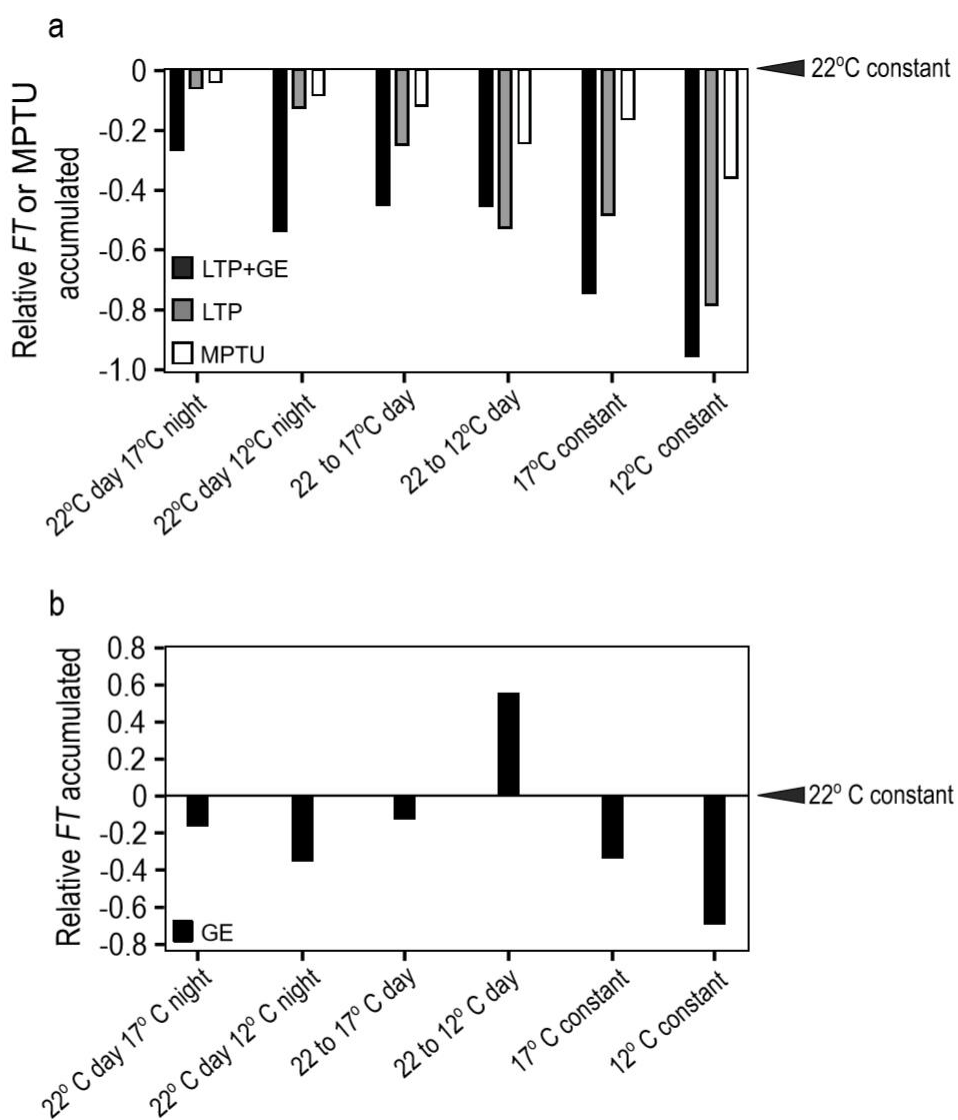


Figure 5

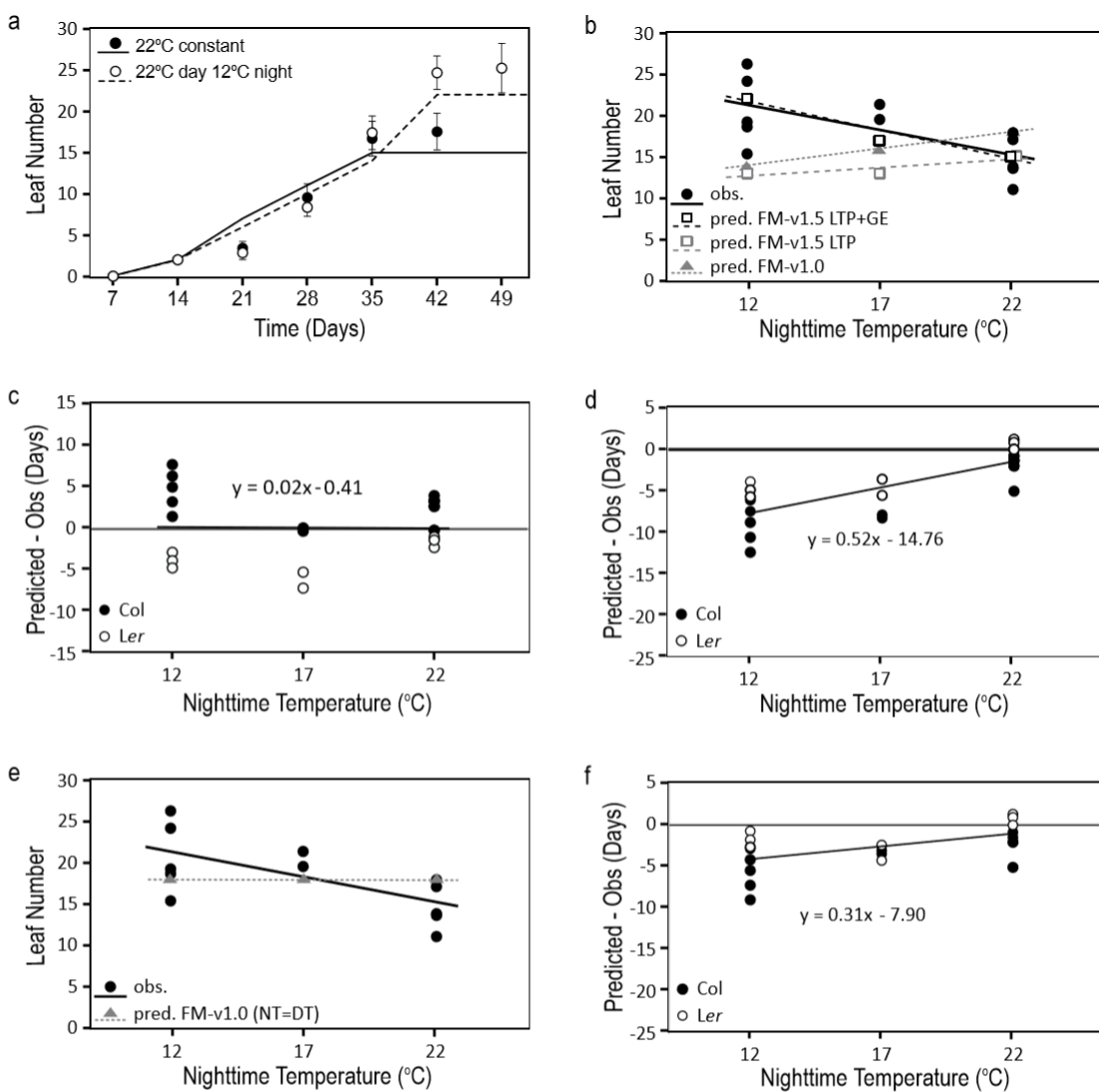


Figure 6

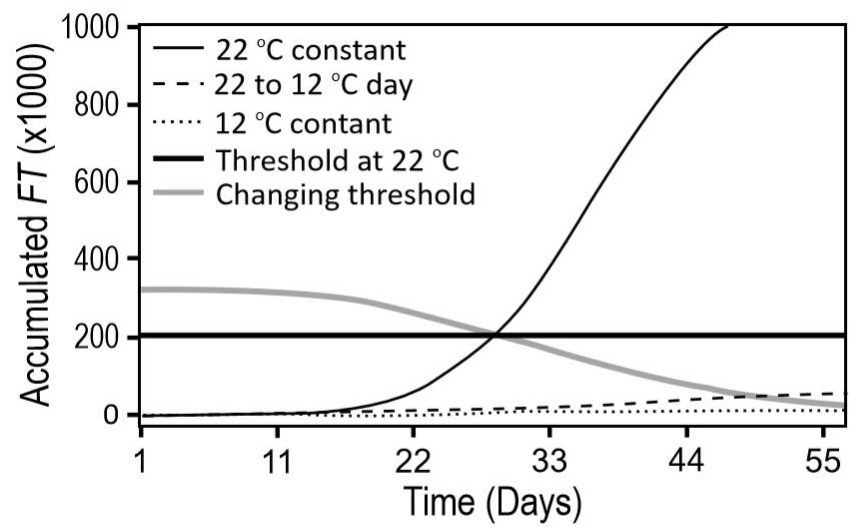


Figure 7

